Development of Monolithic CMOS Pixel Sensors for the ILC at LBNL

M. Battaglia, B. Hooberman, L. Tompkins
Department of Physics, University of California, Berkeley, CA 94720, USA and Ernest Orlando Lawrence Berkeley National Laboratory, Berkeley, CA 94720, USA
J.M. Bussat, D. Contarato, P. Denes, T.S. Kim, T. Stezelberger
Ernest Orlando Lawrence Berkeley National Laboratory, Berkeley, CA 94720, USA

1. INTRODUCTION

The International Linear Collider (ILC) project aims at designing and constructing a machine able to collide e^+e^- beams at center-of-mass energies from $\simeq$ 0.35 TeV up to 1 TeV with luminosities in excess of 10^{34} cm^{-2}s^{-1}. The precise reconstruction of charged particle trajectories close to the interaction region and their extrapolation to the point of origin is a crucial requisite for addressing the broad spectrum of physics questions that we want the ILC to elucidate in the decade after the start of the LHC pp collider at CERN. Detailed simulation studies show that the ILC physics program demands an extrapolation resolution to the beam collision point of the order of 5 (μm) $\oplus$ 10 (μm)$/p_t$ (GeV). This requirement drives the cell size and sensor thickness. While the physics interaction rate at the ILC will be low, the production of soft e^+e^- pairs by photons in the strong electric field of the incoming bunch will determine the detector occupancy. In order to keep the confusion rate in the pattern recognition low, it is necessary to read at least the first layer of the vertex detector within 25 μs. These figures drive the specifications of sensors for application in the ILC vertex tracker, which exceed those developed for current collider experiments by factors of 2 to 50. Several technologies and architectures have been proposed to match these requirements and a significant R&D effort is underway to develop sensor prototypes which can achieve the required performances. Among other technologies, CMOS monolithic pixel sensors adapted for particle tracking applications have been first proposed in [1]. Their main advantage comes from the use of commercially available CMOS technologies, which allow the integration of a highly granular sensor and its readout and signal processing electronics on the same silicon substrate, at a moderate cost. At the same time, the use of a thin epitaxial layer as sensitive volume gives the possibility of achieving a very low material budget by back-thinning the silicon substrate [2].

We report the first results of the R&D program, started at LBNL in 2005, to contribute to the development of a CMOS monolithic pixel sensor suited for the ILC Vertex Tracker. This paper is organized as follows: in Section 2 we describe the design of the first two test structures developed and in Section 3 the data analysis and simulation software. The results of the laboratory tests of the first test structure are discussed in Section 4 and those from exposure to particle beams are in Section 5, where both the test with 1.5 GeV electrons at the LBNL Advanced Light Source (ALS) and with 30 MeV protons at the BASEF facility at the 88-inch Cyclotron are described. Section 6 has the conclusions and the future plans of the R&D program.

2. PIXEL TEST STRUCTURES

2.1. 3T Pixels, different pixel sizes, analog output

A first CMOS pixels prototype was fabricated in 2005 using an AMS 0.35 μm 4-metal, 2-poly CMOS-OPTO technology, which provides an epitaxial layer with a nominal thickness of 14 μm. The chip contains three active pixel arrays, with conventional three transistor pixels with pitches of 10, 20 and 40 μm. The pixels are identical in all three arrays, with a fixed size of the charge-collecting diode of 3 μm and centered within the pixel pitch. The chip has five outputs, which represent any five contiguous pixels. Row and column select logic allows the readout of any five adjacent pixels in a given row.

2.2. 3T Pixels, 20×20 μm^2 pixels, in-pixel CDS, analog output

A second generation of this chip is being designed, also for the AMS 0.35-OPTO process. This new version features a more complex pixel, incorporating circuitry to perform in-pixel correlated double sampling (CDS). Pixels are arrayed on a 20 μm pitch, which allows different collection diode sizes to be tested. Unlike the previous chip, this chip includes the option for a rolling shutter, so that a central region of pixels will be readout at high rate via rolling shutter and the periphery will utilize multiplexed addressing, like the previous version.

3. DATA ANALYSIS AND SENSOR SIMULATION

The first test structure provides an analog signal, then digitised with a 14-bit ADC on a custom readout board equipped with a programmable Xilinx FPGA module, to generate the reset and other signals steering the chip readout sequence. Data is stored on a RAM module and read out through a PCI I/0 card controlled by a LabView online program. This program performs pedestal and noise calculation. The data analysis is performed offline by a dedicated C++ program. Events are first scanned for noisy pixels. Noise and pedestal values are computed by the program if no initialisation has been performed online. Otherwise their values are updated, using the algorithm in [3], to follow possible variations in the course of a data taking run.

Cluster search is performed next. Each event is scanned for pixels with pulse height over a signal-to-noise (S/N) threshold, these are designated as cluster 'seeds'. Seeds are then sorted according to their pulse height values and the surrounding, neighboring pixels are tested for addition to the cluster. The S/N thresholds have been optimized based on running conditions: typically the seed threshold is set at S/N of at least 5 and the neighbor threshold has a S/N of 3. The neighbor search is performed in a 5×5 or 7×7 matrix. Clusters are not allowed to overlap, i.e. pixels already associated to one cluster are not considered for populating another cluster around a different seed. Finally, we require that clusters are not discontinuous, i.e. pixels associated to a cluster cannot be interleaved by any pixel below the neighbor threshold.

After cluster reconstruction, the distance to the nearest cluster and the cluster shape are determined. The cluster shape is characterised by the multiplicity projected over the major and minor axis of the cluster and allows to identify asymmetric clusters, possibly due to inclined tracks or delta rays.

The response of the detector in the beam test has been extensively studied using simulation. Particle tracking and generation of charge is treated using the `Geant 4` package. We have used the Mokka simulation program developed for the ILC full detector simulation [4]. The charge collection process is described in a dedicated module developed within the Marlin reconstruction framework starting from the simulation of individual ionisation points along the particle trajectory and modelling the diffusion of charge carriers from the epitaxial layer to the collection diode. The diffusion coefficient is treated as a free parameter, thus accounting also for inter-pixel capacitive couplings, and has been adjusted to fit the measured pixel multiplicity in clusters. The cluster reconstruction software has been ported to the Marlin framework, running on data converted into the standard LCIO format [5]. This way, beam test and simulated data have been analysed within the same framework and with the same code. The response to 1.5 GeV electrons has been simulated and a rather good agreement has been found with the data taken at the ALS (see Figure 1). The single point resolutions have been computed for the simulated data and again results agree with those inferred from the laser scan (see Section 4.2).

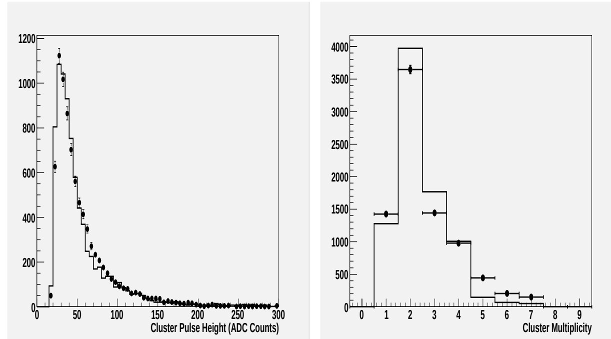

Figure 1: Comparison of measured and simulated response of 10×10 μm pixels to 1.5 GeV e^- beam: (left) cluster pulse heigh and (right) cluster pixel multiplicity

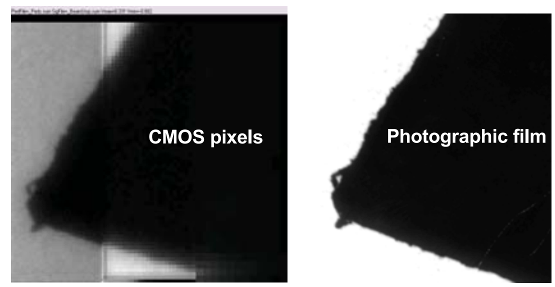

Figure 2: Left: beam stop image with the CMOS pixel structure at a 200 keV electron microscope. Right: same image taken with standard photographic film.

4. SENSOR CHARACTERIZATION

4.1. Electron Microscope Test

The sensor was first tested at the National Center for Electron Microscopy (NCEM) with a 200 keV electron microscope. Figure 2 shows an image of a beam stop, opaque to 200 keV e^-. The triangular hole visible on both images has a base, measured directly on a photographic film image of 25 μm, clearly demonstrating the micrometric pointr spread function of our pixel device in the 10 μm pixel section.

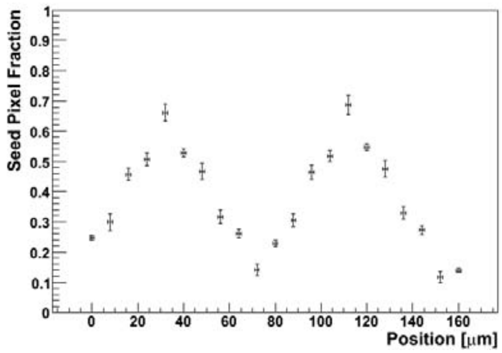

Figure 3: η distribution as a function of the spot position, for the 40×40 μm^2 pixel sector. The two peaks correspond to the position of two pixels, separated by a distance of 80 μm.

4.2. Laser Scans

The analog signal allows to perform a charge center-of-gravity reconstruction to improve the determination of the point of impact of the particle track. We have studied the single point spatial resolution of the detector by performing a scan over several pixel rows with an highly collimated IR laser. The setup consists of an 850 nm laser diode pig-tailed to a 6 μm-core optical fiber. This laser beam is focused by an achromatic lens doublet which provides a spot of the order of 10 μm on the focal plane. The spot position and the distance from the detector plane are controlled to sub-μm accuracy by computer-controlled stages. The 850 nm laser has a short penetration depth in Silicon and therefore minimal charge spreading, allowing to focus most of the incident power onto a single pixel. The stepping motor is used to move the incident beam laterally across the detector surface over a total distance of 4 times the pixel pitch in increments of one fifth of the pixel pitch. This scan is repeated for the three sectors, with pixel pitch of 10, 20 and 40 μm. Figure 3 shows the distribution of the $\eta = \frac{PH_{max}}{PH_{total}}$ distribution, where PH_{max} denotes the pulse height measured on the highest pixel and PH_{total} that of the total cluster, for the sector with 40 μm pixel pitch.

The η distribution is parametrised by a polynomial function and the spatial resolution is extracted by Monte Carlo assuming a uniform distribution of the particle point of impact and the S/N values measured in the beam test. This procedure indicates a resolution of 2.0, 3.3, and 5.1 μm for the sectors with pixel pitches 10, 20, and 40 μm, respectively (see Table I). This agrees well with the resolutions expected from the Geant-4 simulation which are 1.5, 3.2, and 5.5 μm.

Table I ALS Test Beam Results

Pixel Pitch	**10 μm**	**20 μm**	**40 μm**
$<$ Nb of Pixels $>$	2.71	2.67	2.37
$<$ S/N $>$	14.1	14.5	15.4

5. SENSOR RESPONSE TO PARTICLE BEAMS

5.1. Electron beam test

The detector response to high energy particles has been tested using the 1.5 GeV electron beam extracted from the booster ring at the ALS. The beam spill consists of a single bunch with a repetition rate of 1 Hz. The beam intensity can be controlled by varying the electron gun bias and the focusing magnet settings of the BTS beamline; for our tests we adopted two sets of parameters, one providing low intensity (of order of 2 particles mm^{-2}) and high intensity (of order of 20 particles mm^{-2}). The chip reset and readout cycles have been synchronized with the 1 Hz extraction signal from the booster ring, providing reliable timing without the need of using a trigger detector. The chip is kept in reset for most of the time outside the beam spill. For each bunch we then perform a sequence of four reset and frame readout cycles, syncronised so that the beam hits the detector on the third frame. The other, empty frames are used for updating the noise and pedestal levels.

During offline analysis, we select symmetric clusters separated by five or more pixels from the nearest cluster. The results in terms of the average number of pixels in a cluster and the cluster S/N values are summarised in Table I. Using the width of the Landau distribution fitted to the cluster pulse heigh distribution we estimated the equivalent active Si thickness. We compared the data to the predictions of a thin straggling function [6] for different active thicknesses and observe the best agreement for a value of 10 μm (see Figure 4). This thickness corresponds to a most probable energy loss of 1.86 keV or 505 e^-.

5.2. Low Energy Proton beam test

Prior to the irradiation test, described in the next Section, a sample of data was acquired using a low intensity 30 MeV proton beam. In comparison with the results from the electron test described in the previous section, a much larger cluster multiplicity, and a correspondingly larger total cluster signal was found for proton hits. An example of signal distribution is shown in Figure 5.

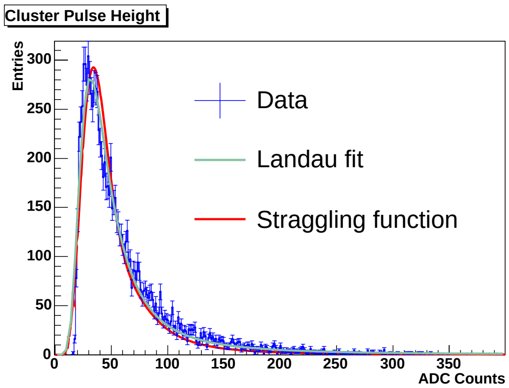

Figure 4: Comparison of ALS data to a Landau function and a thin straggling function. Best agreement is found for a Si thickness of 10 μm.

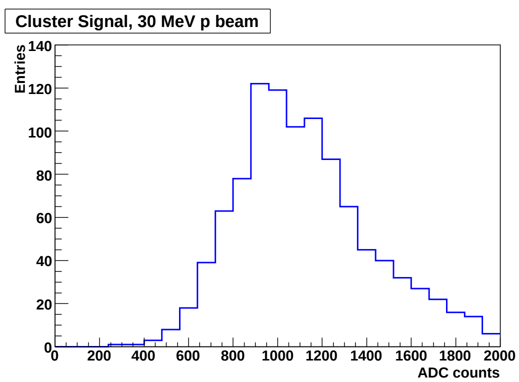

Figure 5: Signal distribution as obtained on 10 μm pitch pixels with 30 MeV protons.

5.3. Irradiation test

An irradiation test was performed with 30 MeV protons at the BASEF facility at the LBNL 88-inch Cyclotron. The detector was mounted on the proton beamline, behind a 2.5 cm diameter collimator, while the readout electronics was placed apart from the beam-line and shielded.

The irradiation was performed in several steps with a 10^7 p cm^{-2} s^{-1} flux, the sensor pedestal and noise values were recorded after each step with the beam off. The total integrated fluence delivered on the detector was 1.45×10^{12} p/cm^2, for a dose equivalent to several years of operation at the ILC at the position of the first layer of the Vertex Tracker. During irradiation, the sensor was always kept under operational conditions, while after irradiation it was stored at room temperature for about 2 weeks. Its performance was tested again both in the laboratory and with the ALS 1.5 GeV e^- beam.

After irradiation the sensor was still functioning with a significant increase of the pedestal levels (see

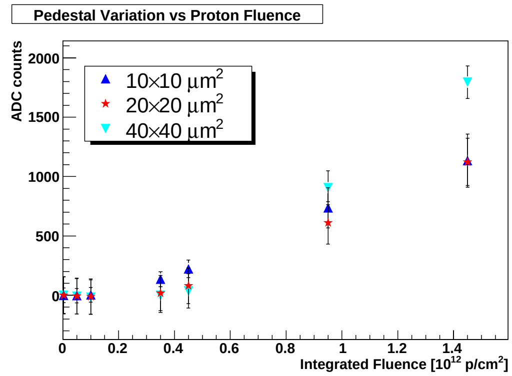

Figure 6: Pedestal variation for the three sensor sectors (10, 20 and 40 μm pitch) as a function of the increasing proton fluence.

Figure 6). An approximately linear trend is followed in all cases, with the largest slope observed for the 40 μm pixels. This suggests a predominant contribution of the pixel leakage current on the pedestal levels. Correspondingly, the pixel noise increases with the proton fluence reaching values $\sim$2-3 times larger than before irradiation.

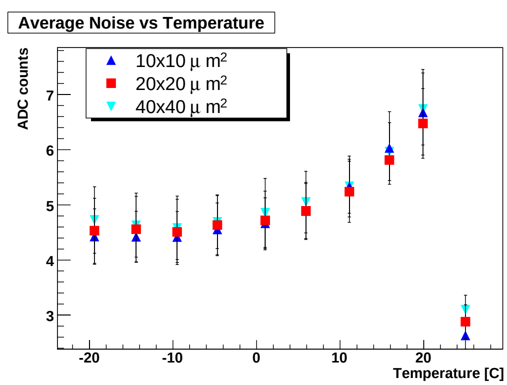

Figure 7: Noise variation for the three sensor sectors (10, 20 and 40 μm pitch) as a function of the operational temperature. The pre-irradiation noise level at room temperature is also indicated.

The performance of the irradiated sensor was then studied as a function of the operational temperature, in a range between +20°C and -25°C. The original noise performance is only partially recovered by operating at low temperature (see Figure 7). This may be explained either as a radiation-induced variation of the sensor gain or as a non-reversible noise contributions, e.g. coming from stable interface states between Silicon and oxide at the detector surface.

The test of the irradiated sensor with 1.5 GeV electrons showed that the sensor retained acceptable particle detection capabilities, despite the increased leakage current. Indeed, the short integration time of 1 ms prevents the pixel output from saturating during the readout cycle. A degradation of the sensor S/N performance was observed, and the average cluster multiplicity was also found to be smaller than before irradiation, possibly due to an increased effect of trapping on the diffusing charge.

6. CONCLUSIONS AND OUTLOOK

Recent results obtained by the LBNL R&D program on CMOS monolithic pixels for the ILC vertex tracker have been reviewed. A first test structure has been designed and tested. The sensor imaging capabilities have been verified using the 200 keV e^- at an electron microscope, while particle detection capabilities have been studied on the a 1.5 GeV e^- beam at the ALS. Additionally, the sensor spatial resolution was extracted from measurements performed with a collimated laser. Beam test data have been compared with sensor simulation performed within the ILC C++ simulation framework.

A first irradiation test was performed with 30 MeV protons, up to doses comparable with the ILC expectations. After irradiation, the sensor was still operational with a degradation of its noise performance, which could be partially recovered by means of moderate cooling.

The next steps of our R&D program include a characterisation of sensor response to low momentum electrons, to validate the simulation results for pair backgrounds, the design and test of more advanced prototypes, implementing data reduction, digitization and sparsification functionalities. A second test structure featuring different architectures for the pixel readout and CDS will be available in Summer 2006 and design studies for a larger size, fast readout prototype with integrated ADCs have been started with the aim of obtaining the chip by mid-2007.

Acknowledgments

This work was supported by the Director, Office of Science, of the U.S. Department of Energy under Contract No. DE-AC02-05CH11231. We are indebted to the staff of the ALS and 88” cyclotron for their help and the excellent performance of the machines. We are also grateful to F. Bieser for his help with the data acquisition board, to H. Matis for the online software and to A. Belkacem with the BTS beamline.

References

[1] R. Turchetta *et al.*, *Nucl. Instr. and Meth. in Phys. Res.* **A458** (2001), 677.
[2] M. Battaglia *et al.*, these Proceedings.
[3] V. Chabaud *et al.*, *Nucl. Instr. and Meth. in Phys. Res.* **A292** (1990), 75.
[4] P. Mora de Freitas and H. Videau, LC-TOOL-2003-010 *Prepared for International Workshop on Linear Colliders (LCWS 2002), Jeju Island, Korea, 26-30 Aug 2002*
[5] F. Gaede, T. Behnke, N. Graf and T. Johnson, eConf **C0303241**, TUKT001 (2003) [arXiv:physics/0306114].
[6] H. Bichsel, *Rev. Mod. Phys.* **60** (1988), 663.